^{18}F-FDG Accumulation with PET for Differentiation Between Benign and Malignant Lesions in the Thorax

Yoshiki Demura, MD[1]; Tatsuro Tsuchida, MD[2]; Takeshi Ishizaki, MD[3]; Shiro Mizuno, MD[1]; Yoshitaka Totani, MD[1]; Shingo Ameshima, MD[1]; Isamu Miyamori, MD[1]; Masato Sasaki, MD[4]; and Yoshiharu Yonekura, MD[5]

[1]Third Department of Internal Medicine, Fukui Medical University, Fukui, Japan; [2]Department of Radiology, Fukui Medical University, Fukui, Japan; [3]Department of Fundamental Nursing, Fukui Medical University, Fukui, Japan; [4]Second Department of Surgery, Fukui Medical University, Fukui, Japan; and [5]Biomedical Imaging Research Center, Fukui Medical University, Fukui, Japan

Recent reports have indicated the value and limitations of ^{18}F-FDG PET and ^{201}Tl SPECT for determination of malignancy. We prospectively assessed and compared the usefulness of these scintigraphic examinations as well as ^{18}F-FDG PET delayed imaging for the evaluation of thoracic abnormalities. **Methods:** Eighty patients with thoracic nodular lesions seen on chest CT images were examined using early and delayed ^{18}F-FDG PET and ^{201}Tl-SPECT imaging within 1 wk of each study. The results of ^{18}F-FDG PET and ^{201}Tl SPECT were evaluated and compared with the histopathologic diagnosis. **Results:** Fifty of the lesions were histologically confirmed to be malignant, whereas 30 were benign. On ^{18}F-FDG PET, all malignant lesions showed higher standardized uptake value (SUV) levels at 3 than at 1 h, and benign lesions revealed the opposite results. Correlations were seen between ^{18}F-FDG PET imaging and the degree of cell differentiation in malignant tumors. No significant difference in accuracy was found between ^{18}F-FDG PET single-time-point imaging and ^{201}Tl SPECT for the differentiation of malignant and benign thoracic lesions. However, the retention index (RI) of ^{18}F-FDG PET (RI-SUV) significantly improved the accuracy of thoracic lesion diagnosis. Furthermore, ^{18}F-FDG PET delayed imaging measuring RI-SUV metastasis was useful for diagnosing nodal involvement and it improved the specificity of mediastinal staging. **Conclusion:** No significant difference was found between ^{18}F-FDG PET single-time-point imaging and ^{201}Tl SPECT for the differentiation of malignant and benign thoracic lesions. The RI calculated by ^{18}F-FDG PET delayed imaging provided more accurate diagnoses of lung cancer.

Key Words: ^{18}F-FDG PET; ^{201}Tl SPECT; retention index; lung cancer; nodal staging

J Nucl Med 2003; 44:540–548

Received Jul. 17, 2002; revision accepted Oct. 24, 2002.

For correspondence or reprints contact: Yoshiki Demura, MD, Third Department of Internal Medicine, Fukui Medical University, 23 Matsuoka-cho, Fukui Pref 910-11, Japan.

E-mail address: DEM2180@aol.com

Conventional radiologic assessment (chest radiography, CT, MRI) of thoracic abnormalities is being complemented by PET, which is becoming known as a powerful tool. In the thorax, PET has been used to evaluate tumor imaging. ^{18}F-FDG, a D-glucose analog labeled with ^{18}F used as a radiopharmaceutical, is ideally suited for tumor imaging (*1*,*2*). Many reports have indicated that ^{18}F-FDG PET is sensitive and specific for the diagnosis and staging of several types of malignancies (*3*–*5*); however, ^{18}F-FDG accumulation is not specific to malignancies because there are numerous causes of ^{18}F-FDG uptake in benign processes (*6*–*8*). As the result, increased ^{18}F-FDG uptake in lesions such as benign tumors or inflammatory processes leads to false-positive results and misdiagnoses of malignancies (*9*,*10*). It has also been reported that ^{201}Tl accumulations on SPECT differ between benign and malignant tumors (*11*,*12*). ^{201}Tl SPECT is often used for the evaluation of malignancies because it is more cost efficient and more widely available than ^{18}F-FDG PET. Furthermore, ^{201}Tl accumulation is seen in malignant tumors on both early and delayed scans; however, it is not seen on delayed scans in the case of benign tumors. Therefore, retention of ^{201}Tl on a delayed scan is strongly suggestive of malignancy (*13*).

Various cell types exhibit varying rates of ^{18}F-FDG uptake and metabolism, and we hypothesized that measurements at 2 time points may prove to be helpful in differentiating malignant from benign diseases and that ^{18}F-FDG PET is superior to ^{201}Tl SPECT in terms of disease specificity. Therefore, we tested our hypothesis by assessing the results of dual-time-point ^{18}F-FDG PET imaging. Furthermore, we performed a comparison of ^{18}F-FDG PET and ^{201}Tl SPECT in patients with thoracic abnormalities to validate the usefulness of ^{18}F-FDG PET delayed imaging.

MATERIALS AND METHODS

Subjects

We studied 80 patients (49 men, 31 women; age range, 23–80 y; mean age, 65.0 ± 11.9 y) with thoracic abnormalities suspected to be thoracic malignancy—that is, lung cancer—on the basis of chest CT results. All patients underwent preoperative ^{18}F-FDG PET and ^{201}Tl SPECT examinations between October 1998 and April 2002, and the respective studies were completed within 1 wk of each other. All patients underwent a thoracotomy, open lung biopsy, or lung biopsy using video-assisted thoracoscopic surgery within 4 wk of the ^{18}F-FDG and ^{201}Tl examinations. All lesions were removed completely and examined histologically. Three patients with abnormal pulmonary shadows that disappeared or were reduced before surgery were diagnosed as having organizing pneumonia on the basis of results of a transbronchial lung biopsy and clinical follow-up. Another 3 patients were diagnosed with mycobacterial infection on the basis of positive results of a bacteriologic examination through bronchial lavage and clinical follow-up. All cases of tuberculosis and all designators of mycobacteria were proven by bacteriologic examination. Informed consent was obtained from all patients participating in the study.

^{18}F-FDG PET

^{18}F-FDG PET imaging was performed using a whole-body scanner (ADVANCE; General Electric Medical Systems, Milwaukee, WI). After at least 4 h of fasting, each subject underwent transmission scanning for attenuation correction for 10 min. Immediately after obtaining the transmission scan, 370 MBq ^{18}F-FDG were intravenously administered, and static scans were obtained 1 h later for 10 min and 3 h later for 20 min. Only 1 preinjection transmission scan was acquired. In each emission scan, the patient's body was carefully positioned with the guidance of a laser beam so that misregistration should not occur. Images were then reconstructed and viewed as transaxial slices of the chest and coronary slices of the whole body, with a slice thickness of 7 mm. Between the early and delayed scans, patients returned to their hospital room and waited quietly. CT was performed on all patients before ^{18}F-FDG PET. On the basis of this information and the transmission scan, we can ensure that the tumor is in the field of view. ^{18}F-FDG and ^{201}Tl images were interpreted visually from the films and correlated carefully with the CT results at the same time. For qualitative analysis, any obvious foci of increased ^{18}F-FDG or ^{201}Tl uptake over the background were considered positive for a tumor. For semiquantitative analysis of the ^{18}F-FDG uptake, a standardized uptake value (SUV) (tumor activity concentration/injected dose/body weight) measurement was obtained at the most active tumor site by drawing a region of interest (ROI) around the lesion that encompassed all pixels with uptake values of >90% of the maximum uptake in the transaxial slice, after which the average counting rate in each ROI was calculated. The SUV was calculated using a calibration factor between PET counts and radioactivity concentration. Primary lung lesions with an SUV of <2.5 or undetectable in early imaging and delayed imaging were considered benign. Furthermore, we calculated the retention index (RI-SUV) from the results of 1-h (early scan) and 3-h (delayed scan) imaging according to the following equation: RI-SUV (%) = (SUV [delayed scan] − SUV [early scan]) × 100/SUV (early scan). If the RI (SUV) of ^{18}F-FDG was positive, the thoracic lesion was considered to be malignant by the results of RI-SUV. To assess nodal disease, all pulmonary and mediastinal malignancies were analyzed visually and considered positive if the ^{18}F-FDG accumulation had increased relative to that in the adjacent mediastinal and soft-tissue structures in the early imaging. Furthermore, the RI of positive lymph nodes was calculated according to delayed imaging, and, if positive, nodal involvement was considered positive in the delayed imaging (RI) study. Nodal (N) staging was diagnosed according to pathologic findings. The results of ^{18}F-FDG PET were expressed from early imaging, delayed imaging, and RI results and then compared among them.

If the results of ^{18}F-FDG PET can be positive for malignancy or negative for benign disease, we considered that they should be accurate diagnoses and calculated the accuracy from the ratio of total cases.

^{201}Tl SPECT

All patients were examined by ^{201}Tl SPECT within 1 wk of the PET study. With the subjects at rest, 111 MBq ^{201}Tl-chloride were injected into a peripheral vein, and imaging was performed after 15 min (early scan) and 3 h (delayed scan). SPECT was performed using a rotating gamma-camera system (GCA-9300A/HG; Toshiba, Tokyo, Japan) with a slice thickness of 5.8 mm. For semiquantative analysis of ^{201}Tl SPECT, an ROI was defined manually on transaxial tomograms that showed the highest uptake of the lesion to be in the middle of the tumor. The ROI placed on the lesion encompassed all pixels that had uptake values of >90% of the maximum uptake in that slice, and the average counting rate in each ROI was calculated. Radioactivity was also measured for areas of the homologous contralateral normal lung to calculate the tumor-to-normal lung ratio (T/N) of the activity on early scans (early ratio [ER]) and on delayed scans (delayed ratio [DR]). The RI of ^{201}Tl was also calculated for tumor activity according to the following equation: RI-Tl (%) = (DR-ER) × 100/ER.

If the RI of ^{201}Tl was positive, the thoracic lesion was considered to be malignant, whereas all undetectable cases were considered benign. ^{201}Tl SPECT images of all pulmonary and mediastinal malignancies were classified as positive for nodal involvement when there was at least 1 area of definitely increased radioactivity in the mediastinum, other than areas in the myocardium and thoracic spine. When there was no uptake of ^{201}Tl in the mediastinum or when the accumulation was equivocal or could not be distinguished from that in the myocardium or vertebra, the images were considered negative (*12*). We also assessed the clinical accuracy compared with the pathologic diagnosis.

Thoracic CT

CT scans were obtained using a helical CT system (HiSpeed Advantage RP; General Electric Medical Systems). Contiguous 1-cm-thick sections were obtained at 1-cm intervals from the lung apices to the adrenal glands before and during intravenous bolus injection of contrast material at 2 mL/s by a power injector. Results of nodal staging were classified as either positive or negative on the basis of the presence or absence of mediastinal node enlargement, which was defined as a node of >1 cm in short-axis diameter on transaxial images. Results of the scans were correlated with the pathologic diagnosis.

Radiographic images were interpreted independently and prospectively by experienced radiologists and nuclear medicine physicians, without knowledge of histopathologic or other radiologic data.

Statistical Analysis

Results of ^{18}F-FDG (uptake, RI) and ^{201}Tl (uptake, RI) are expressed as mean ± SD. Differences in ^{18}F-FDG uptake between

the early (1 h) and delayed images (3 h), as reflected by SUV levels, were examined for statistical significance using the Wilcoxon signed rank test. Comparisons of differences between the results of ^{18}F-FDG (SUV level, RI) or ^{201}Tl uptake (T/N ratio, RI) were performed with 1-way ANOVA using the Fisher protected least-significant difference (PLSD). The diagnostic accuracy of PET and ^{201}Tl SPECT was compared by a McNemar test. Any correlation between the 2 variables was analyzed with the Pearson coefficient of correlation. $P < 0.05$ was considered to be statistically significant.

RESULTS

Subject Demography and Clinical Characteristics

All malignancies (50 cases) and benign lesions (24 cases) were histologically confirmed by surgical resection. Three patients with abnormal pulmonary shadows that disappeared or were reduced before surgery were diagnosed as having organizing pneumonia on the basis of results of a transbronchial lung biopsy and clinical follow-up. Another 3 patients were diagnosed with a mycobacterial infection on the basis of positive results of a bacteriologic examination through bronchial lavage and clinical follow-up. The thoracic lesions ranged in size from 11 to 60 mm, with most lesions < 30 mm in diameter. The radionuclide examination results and diagnoses for the 80 thoracic lesions are summarized in Table 1.

^{18}F-FDG PET and ^{201}Tl SPECT in Thoracic Lesions

We observed all malignant tumors (malignant disease group) that exhibited a higher SUV level at 3 than at 1 h (Fig. 1A) ($P < 0.0001$, analyzed by Wilcoxon signed rank test). Benign lesions, with the exception of those with granulomatous disease (benign disease group), showed significantly lower SUV levels at 3 than at 1 h (Fig. 1B) ($P = 0.0007$, analyzed by Wilcoxon signed rank test), whereas all mycobacterial infections and 1 case of nodular sarcoidosis (granulomatous disease group) exhibited a higher SUV level at 3 than at 1 h (Fig. 1C) ($P = 0.0051$, analyzed by Wilcoxon signed rank test). The correlation between SUV level (1 h, 3 h, and RI-SUV) and degree of cell differentiation in thoracic malignancies is seen in Figure 2. Furthermore, the SUV levels at 1 and 3 h of well-differentiated adenocarcinoma and well-differentiated squamous cell carcinoma were significantly lower than those of poorly differentiated adenocarcinoma ($P = 0.0003$ at 1 h and $P = 0.0001$ at 3 h, analyzed by the Fisher PLSD) and poorly differentiated squamous cell carcinoma ($P = 0.0002$ at 1 h and $P < 0.0001$ at 3 h, analyzed by the Fisher PLSD). RI-SUV results were the same. Moreover, undifferentiated carcinoma (small cell carcinoma and large cell carcinoma) had a higher index (RI-SUV) than low-grade malignant diseases (carcinoid and mucosa-associated lymphoid tissue lymphoma) ($P = 0.0012$, analyzed by the Fisher PLSD). Representative cases of ^{18}F-FDG PET delayed imaging for differential diagnosis of well-differentiated adenocarcinoma are shown in Figure 3 and benign lesions are shown in Figure 4. In contrast, no significant differences were found among ^{201}Tl ER, DR, and RI (Fig. 5).

The diagnostic values of ^{18}F-FDG PET (early image, delayed image, and RI-SUV) and ^{201}Tl SPECT were evaluated for thoracic lesions (Table 2). According to the results, ^{18}F-FDG PET early image and delayed image and

TABLE 1
Patient Characteristics

Group	Patient no.	Histology (diagnosis)	Size* (cm)	Detection rate (%)	
				^{18}F-FDG PET	^{201}Tl SPECT
1	15	Well-diff. adenoca. including 7 BAC	2.23 ± 0.65	14/15 (93.3)	6/15 (40.0)
2	5	Moderately diff. adenoca.	2.86 ± 0.96	5/5 (100.0)	3/5 (60.0)
3	5	Poorly diff. adenoca.	3.24 ± 1.56	5/5 (100.0)	4/5 (80.0)
4	4	Well-diff. SCC	2.38 ± 0.85	4/4 (100.0)	1/4 (25.0)
5	3	Moderately diff. SCC	3.63 ± 0.91	3/3 (100.0)	3/3 (100.0)
6	8	Poorly diff. SCC	2.91 ± 1.19	8/8 (100.0)	7/8 (87.5)
7	6	Undiff. carcinoma: 3 SCLC, 3 large cell ca.	3.08 ± 1.17	6/6 (100.0)	5/6 (83.3)
8	4	Low-grade malignancy: 3 carcinoid, 1 MALT lymphoma	3.38 ± 1.17	4/4 (100.0)	4/4 (100.0)
9†	20	Benign disease (excluding group 10)	3.48 ± 5.33	15/20 (75.0)	5/20 (25.0)
10‡	10	Granulomatous disease	2.28 ± 0.52	10/10 (100.0)	6/10 (60.0)

*No significant differences among size of each group.

†Group 9 consisted of 1 each of schwannoma of mediastinum, cavernous hemangioma of mediastinum, lymphangioma of mediastinum, leiomyoma of mediastinum, lymphocele of mediastinum, intrapulmonary lymphadenitis (fibrosis and anthracosis of lymph node), lung abscess, and pulmonary amyloidosis (nodular type), along with 5 pulmonary aspergilloses and 7 organizing pneumonia patients.

‡Group 10 consisted of 4 pulmonary tuberculosis, 5 pulmonary atypical mycobacteriosis, and 1 pulmonary sarcoidosis (nodular type) patient.

Diff. = differentiated; adenoca. = adenocarcinoma; BAC = bronchioloalveolar carcinoma; SCC = squamous cell carcinoma; Undiff. = undifferentiated; SCLC = small cell lung carcinoma; large cell ca. = large cell carcinoma; MALT = mucosa-associated lymphoid tissue (low-grade B-cell lymphoma).

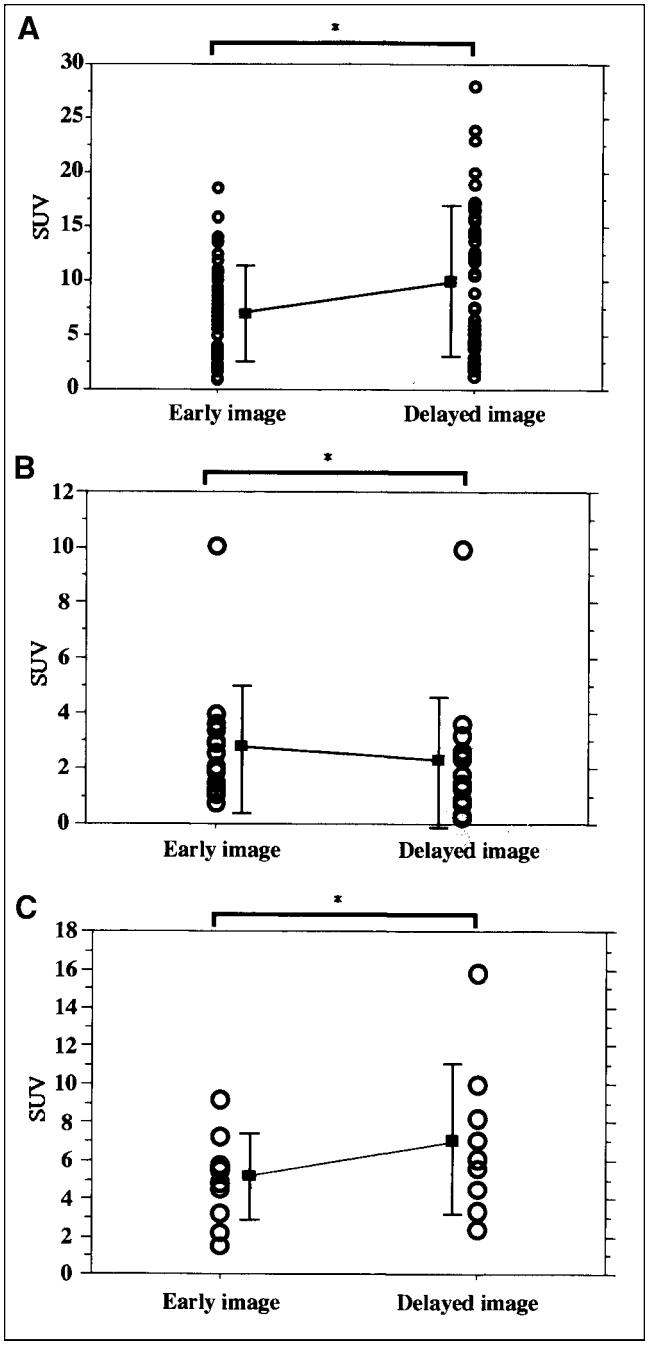

FIGURE 1. Changes in ^{18}F-FDG accumulation (SUV) between early and delayed imaging in primary lesions of malignant lesion group (mostly lung cancer) (A), benign disease group (group 9) (B), and granulomatous disease group (group 10) (C). Significant increases of SUV in A and C and significant decrease of SUV in B were observed. Bars indicate mean ± SD. *$P < 0.05$.

^{201}Tl SPECT showed no differences; however, RI-SUV was significantly superior in distinguishing a benign lesion from a malignant lesion in terms of accuracy (RI-SUV vs. ^{201}Tl SPECT: $P = 0.00558$; RI-SUV vs. PET early image: $P = 0.0001$; RI-SUV vs. PET delayed image: $P = 0.0005$, analyzed by the McNemar test).

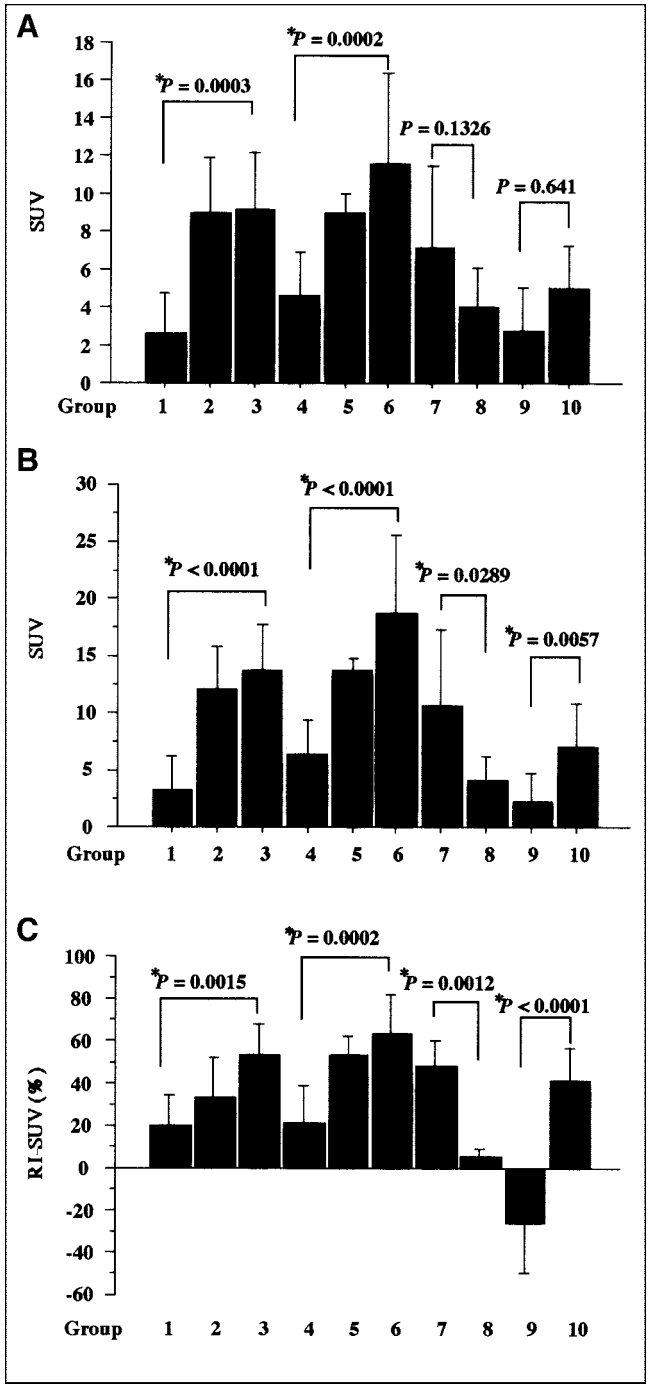

FIGURE 2. Comparison of SUV levels with ^{18}F-FDG PET. (A) Early imaging. (B) Delayed imaging. (C) RI in thoracic lesions. Significant correlations were observed between SUV levels and degree of cell differentiation in lung cancer. For adenocarcinoma, squamous cell carcinoma, and undifferentiated carcinoma, ^{18}F-FDG accumulations in delayed images better reflected degree of cell differentiation than that in early images. For SUV RI, cell differentiation was better reflected and benign disease group (group 9) was significantly differentiated from other groups. Results are expressed as mean ± SD.

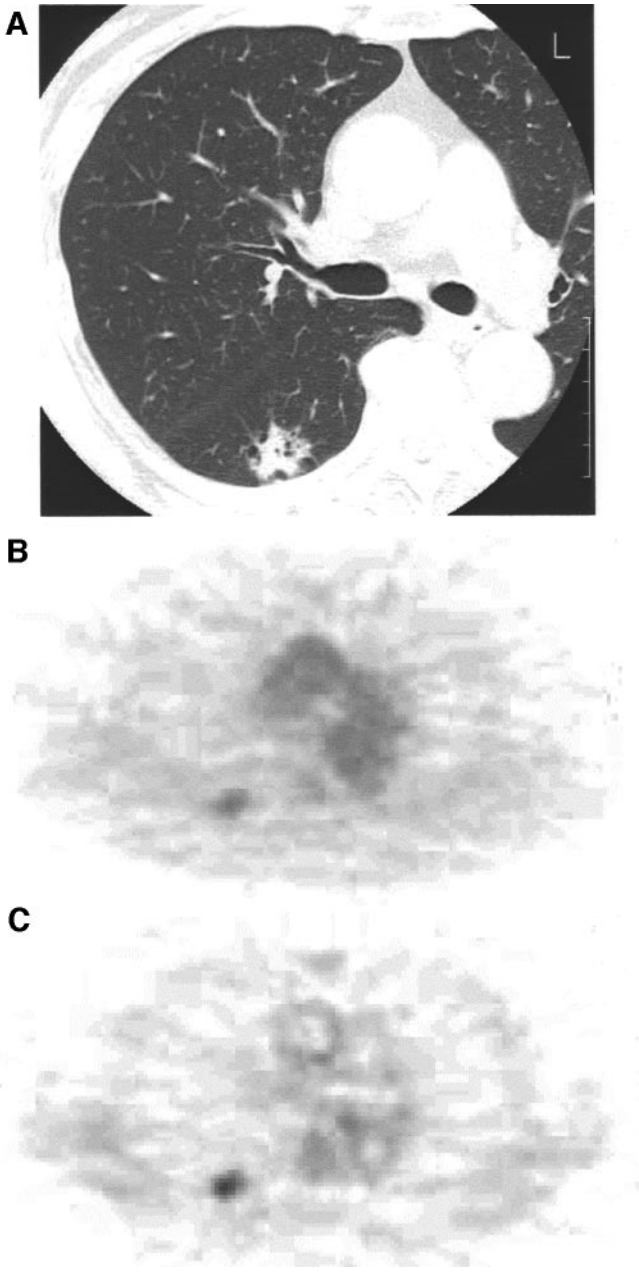

FIGURE 3. Patient with well-differentiated lung adenocarcinoma (2.2 × 2.0 cm). (A) CT image shows nodule in right lung. (B) ^{18}F-FDG PET early image shows faint accumulation in nodule (SUV = 2.40). (C) ^{18}F-FDG PET delayed image shows increased hot accumulation in nodule (SUV = 3.00) along with good visualization. Nodule was not detected by ^{201}Tl SPECT (image not shown).

^{18}F-FDG PET and ^{201}Tl SPECT in Diagnosis of Nodal Staging

In nodal staging, conventional ^{18}F-FDG PET (early imaging) and ^{201}Tl SPECT were more accurate than thoracic CT (Table 3), and ^{18}F-FDG PET imaging showed excellent sensitivity compared with that of other modalities. In the delayed imaging (RI) study, the specificity was significantly improved from 62.9% to 91.4% ($P = 0.0044$, analyzed by the McNemar test). Overall, ^{18}F-FDG PET delayed imaging (RI) was significantly more accurate than the other modalities (PET delayed imaging study vs. CT: $P = 0.0004$; PET delayed imaging study vs. ^{201}Tl SPECT: $P = 0.009$; PET delayed imaging study vs. PET early imaging: $P = 0.003$, analyzed by the McNemar test). Furthermore, a close correlation between the RI-SUV results of the primary lesion and lymph node metastasis was observed (Fig. 6), which was helpful in the diagnosis of nodal staging.

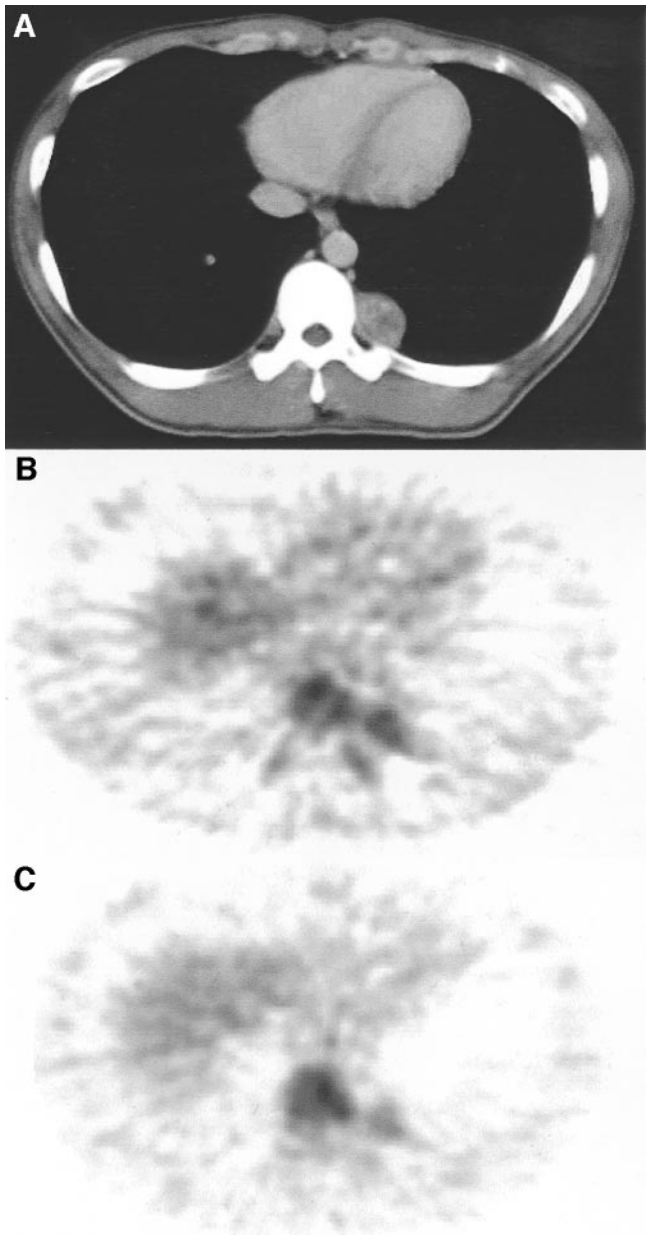

FIGURE 4. Patient with posterior mediastinal schwannoma (3.5 × 2.2 cm). (A) CT image shows nodule in left thorax. (B) ^{18}F-FDG PET early image shows hot accumulation in nodule (SUV = 2.80). (C) ^{18}F-FDG PET delayed image shows decreased hot accumulation in nodule (SUV = 1.70). Nodule was not detected by ^{201}Tl SPECT (image not shown).

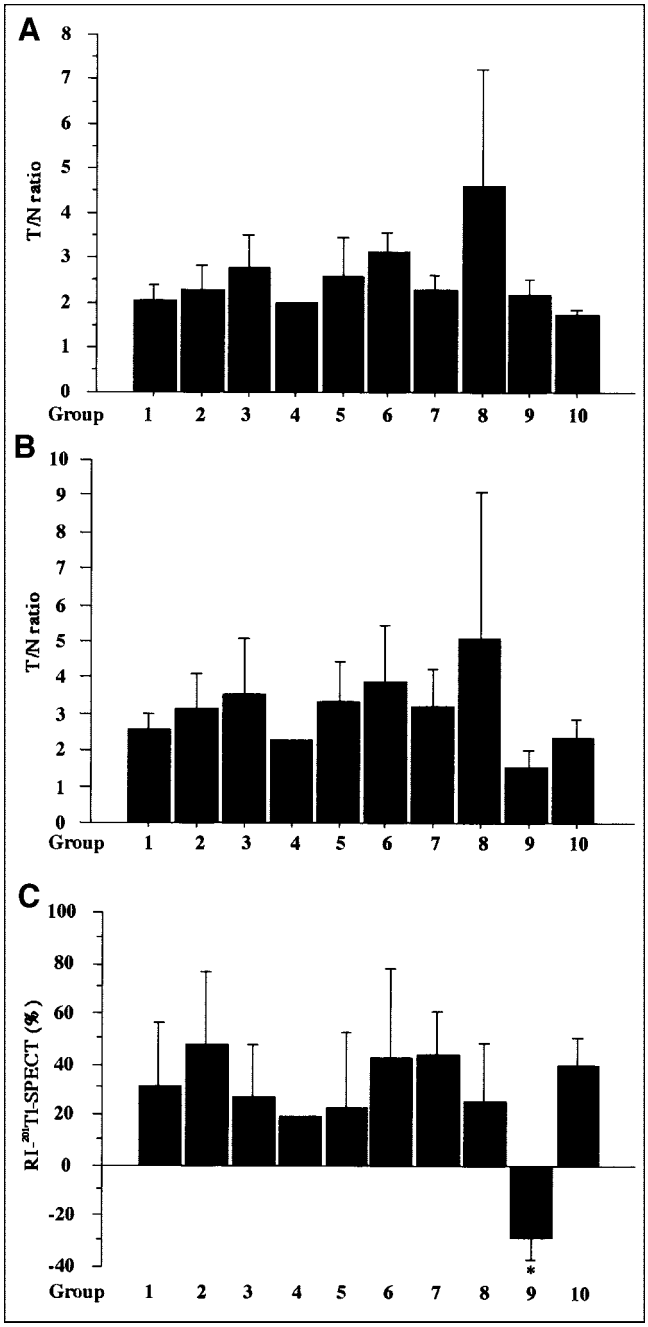

FIGURE 5. Comparison of results of ^{201}Tl SPECT. (A) Early imaging. (B) Delayed imaging. (C) RI in thoracic lesions. No significant correlations were observed between results and degree of cell differentiation in lung cancer. As for RI of ^{201}Tl SPECT, only benign disease group (group 9) was significantly differentiated from others. Results are expressed as mean ± SD. *$P < 0.05$ vs. other groups, excluding group 4.

DISCUSSION

In this study, we compared ^{18}F-FDG PET and ^{201}Tl SPECT, including early images, delayed images, and SUV RI, in evaluations of several kinds of thoracic lesions. As for differentiation between malignant and benign diseases, there were no significant advantages among ^{18}F-FDG PET early and delayed imaging and ^{201}Tl SPECT imaging; however, ^{18}F-FDG PET RI (RI-SUV) was found to be useful and far superior to other scintigraphic techniques, thus improving diagnostic potential. Our results clearly suggest significant advantages of dual-time-point ^{18}F-FDG PET imaging for differentiating malignant lesions from benign lesions, whereas delayed ^{18}F-FDG PET imaging alone may not be helpful for differential diagnosis.

Several studies have shown the advantages of delayed imaging with ^{18}F-FDG, and delayed scans have been reported as useful for the diagnosis of pancreatic cancer and breast cancer (*14*,*15*). Recently, Kubota et al. (*16*) found that ^{18}F-FDG PET 2-h delayed imaging of the whole body easily detected malignant lesions because of the increased uptake by tumors along with a decreased normal background. Zhuang et al. (*17*) also showed differences in the rates of ^{18}F-FDG uptake between malignant and inflammatory mononuclear cells and processes in vitro and suggested that lung lesions with decreased or stable SUVs over time are likely to have a benign etiology, whereas those with increased SUVs over time are likely to be caused by malignancy. Thus, we believe that the results presented in these reports support our clinical data. Actually, the usefulness of dual-time-point ^{18}F-FDG PET imaging for the evaluation of pulmonary nodules was also reported by Matthies et al. (*18*). We consider that their outcomes were quite similar to ours. We selected a 1-h time point for early imaging and a 3-h time point for delayed imaging. Imaging 1 h later seems to be a conventional timing in ^{18}F-FDG PET studies. As for 3-h later imaging, we expected the merit of 3-h later imaging compared with Kubota's 2-h delayed imaging to be that the longer interval brought the larger difference of SUV of the thoracic lesion. The report of Hamberg et al. (*19*) supported our hypothesis. We also had to take into account the decay of radioactivity of ^{18}F-FDG. Then, we decided on the imaging time points 1 and 3 h later.

The accuracy of nodal staging can also be improved by a combination of early and delayed ^{18}F-FDG PET imaging. It is well recognized that the results of current nodal staging procedures in patients with lung cancer are not accurate; even ^{18}F-FDG PET cannot provide sufficient data (*12*,*20*). Furthermore, previous reports have shown the advantages and limitations of ^{201}Tl SPECT and ^{18}F-FDG PET imaging in nodal staging (*10*,*12*). The former is insufficient for sensitivity and the latter is inadequate for specificity of mediastinal staging, although they are better than CT. ^{18}F-FDG accumulation with PET had a high sensitivity for malignancy; however, it also accumulated in many kinds of inflammatory lymph node swelling, reducing the specificity for diagnosis. Our results indicated similar findings as well. However, we found that ^{18}F-FDG PET, including the analysis of RI, could distinguish between benign and malignant lymph nodes because malignant lymph nodal metastasis always increased SUV on delayed images and RI-SUV, whereas most normal tissue—including muscle, mediastinum, or benign lymph node swelling (such as inflammation

TABLE 2
Comparison of ^{18}F-FDG PET (Early Imaging, Delayed Imaging, and RI) and ^{201}Tl SPECT Results for Diagnosis of Malignancy

Thoracic lesion	^{18}F-FDG PET			^{201}Tl SPECT
	Early imaging (%)	Delayed imaging (%)	RI (%)	RI (%)
Low-grade malignancy	2/4 (50.0)	2/4 (50.0)	4/4 (100.0)	3/4 (75.0)
Well-diff. carcinoma	8/19 (42.1)	9/19 (47.4)	18/19 (94.7)	6/19 (31.6)
Moderately diff. carcinoma	8/8 (100.0)	8/8 (100.0)	8/8 (100.0)	7/8 (87.5)
Poorly diff. carcinoma	13/13 (100.0)	13/13 (100.0)	13/13 (100.0)	10/13 (76.9)
Undiff. carcinoma	6/6 (100.0)	6/6 (100.0)	6/6 (100.0)	5/6 (83.3)
Benign disease (including granulomatous disease)	15/30 (50.0)	17/30 (56.7)	20/30 (66.7)	24/30 (80.0)
Sensitivity (%)	74.00	76.00	98.00	63.30
Specificity (%)	50.00	56.70	66.70	80.00
Accuracy (%)	65.0*	68.8*	86.30	68.8*

*$P < 0.01$ vs. RI of ^{18}F-FDG PET.
Diff. = differentiated; Undiff. = undifferentiated.
Accuracy of ^{18}F-FDG PET RI was significantly higher than that of other modalities.

and hyperplasia)—decreased SUV on delayed images and RI-SUV, with the exception of granulomatous inflammation such as sarcoid reaction. In addition, a close correlation between RI-SUV for primary tumors and lymph node metastasis is useful in the diagnosis of nodal involvement. Consequently, this method is considered to improve the specificity of mediastinal staging and provide a new and effective means for staging thoracic lymph nodes in patients with lung cancer, making it superior to other modalities for the assessment of hilar and mediastinal nodal metastases.

It is unclear why inflammatory and malignant lesions exhibit a differential ^{18}F-FDG uptake pattern over time, although several cellular factors may contribute to this phenomenon. It is well known that many cancer cells express increased numbers of glucose transporters (*21*); thus, metabolic trapping through phosphorylation of FDG appears likely to be the rate-determining step for ^{18}F-FDG retention in the cell. Hexokinase and glucose-6-phosphatase mediate the phosphorylation and dephosphorylation, respectively, of intracellular FDG. Unless ^{18}F-FDG-6-phosphate is dephosphorylated by glucose-6-phosphatase, it is unable to leave the cell. Furthermore, it has been shown that most actively proliferating tumor cells have low levels of glucose-6-phosphatase (*22*,*23*). On the basis of these observations, an increased ratio of hexokinase to glucose-6-phosphatase may result in a gradual accumulation of ^{18}F-FDG-6-phosphate. In contrast, most normal tissues express greater levels of glucose-6-phosphatase than malignant cells, whereas mononuclear cells and fibroblast cells, which represent the major cell populations in chronic inflammation, also have a relatively a low ratio of hexokinase to glucose-6-phosphatase (*24*). However, different blood vessel density and flow can have a dramatic influence on ^{18}F-FDG uptake (*25*). Thus, dual-time imaging and the retention of ^{18}F-FDG can more accurately reflect the ratio of hexokinase to glucose-6-phosphatase, indicating cell proliferation potential (*26*,*27*).

Traditionally, a single time point SUV of 2.0–3.0 has been proposed as the optimal threshold for separating malignant from benign lung lesions (*28*,*29*). However, there is considerable overlap between SUV results of malignant and benign lesions, causing difficulty in correctly interpreting ^{18}F-FDG PET data (*30*,*31*). As our results indicated, there is a wide range of ^{18}F-FDG uptake (SUVs = 6.82 ± 4.36)

TABLE 3
Comparison of ^{18}F-FDG PET (Early Imaging, Delayed Imaging, and RI), ^{201}Tl SPECT, and CT Results for Lymph Node Staging of Malignancy (Including 49 Cases of Lung Cancer)

Modality (%)	N0	N1	N2	N3	Sensitivity	Specificity	Overall accuracy
CT	24/35 (68.6)	—	6/13 (46.2)	0/2 (0.0)	5/15 (33.3)	24/35 (68.6)	30/50 (60.0)*
^{201}Tl SPECT	27/35 (77.1)	—	7/13 (53.8)	1/2 (50.0)	8/15 (53.3)	27/35 (77.1)	35/50 (70.0)*
^{18}F-FDG PET							
Early imaging	22/35 (62.9)	—	11/13 (84.6)	2/2 (100.0)	13/15 (86.7)	22/35 (62.9)†	35/50 (70.0)*
Delayed imaging	32/35 (91.4)	—	12/13 (92.3)	2/2 (100.0)	14/15 (93.3)	32/35 (91.4)	46/50 (92.0)

*$P < 0.05$ vs. accuracy of ^{18}F-FDG PET delayed imaging (using RI).
†$P < 0.05$ vs. specificity of ^{18}F-FDG PET delayed imaging (using RI).

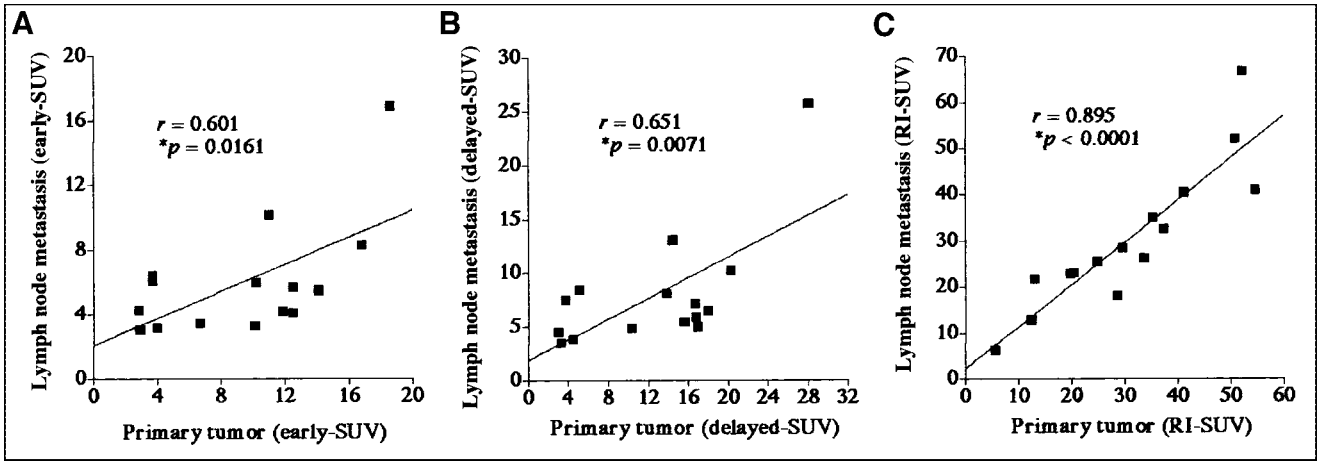

FIGURE 6. (A) Correlation between SUV levels of lymph node metastases and primary tumors in ^{18}F-FDG PET early imaging of lung cancer patients with nodal involvement. Correlation between SUV levels of lymph node metastases and primary tumors was found ($y = 0.418x + 2.113$; $r = 0.601$; $P = 0.0161$). (B) Correlation between SUV levels of lymph node metastases and primary tumors in ^{18}F-FDG PET delayed imaging of lung cancer patients with nodal involvement. Correlation between SUV levels of lymph node metastases and primary tumors was found ($y = 0.482x + 1.894$; $r = 0.651$; $P = 0.0071$). (C) Correlation between RI-SUV (%) of lymph node metastases and primary tumors in ^{18}F-FDG PET early imaging of lung cancer patients with nodal involvement. Good correlation between RI-SUV (%) of lymph node metastases and primary tumors was found ($y = 0.917x + 2.180$; $r = 0.895$; $P < 0.0001$). Result in C showed best correlation among 3 graphs.

among malignant lesions, whereas high SUVs in benign lesions have also been observed, such as for sarcoidosis or amyloidosis, which have SUVs as high as 10. Previous reports, along with our results, have shown that inflammatory and infectious lesions or benign variations can simulate malignant lesions in terms of SUV results (*6–8*). Consequently, SUVs at single time points alone may not be reliable enough to characterize malignant lesions with various pathologies. Therefore, an investigation of alternative methods using ^{18}F-FDG PET for differentiation of malignancy from benign lesions is warranted.

It is known that ^{201}Tl SPECT can differentiate between benign and malignant tumors (*12,13*). Because ^{201}Tl accumulations are seen in malignant tumors on both early and delayed scans—however, not seen on delayed scans of benign tumors—the retention of ^{201}Tl on delayed scans is strongly suggestive of malignancy (*13*). However, we found that ^{201}Tl SPECT had a limitation in sensitivity for small lesions, and findings for both ^{18}F-FDG PET and ^{201}Tl SPECT showed that a positive RI gave false-positive results for the same 6 benign lesions (mycobacterosis). Few reports that have compared ^{18}F-FDG PET and ^{201}Tl SPECT, although Higashi et al. (*32*) recently found no significant differences between them regarding specificity for the differentiation of malignant and benign pulmonary nodules. From their results and our data, the conventional ^{18}F-FDG PET imaging (early imaging) cannot provide sufficient accuracy to overcome the present situation; therefore, we recommend that RI-SUV results of ^{18}F-FDG PET should be used for the diagnosis of unknown lesions because they are able to distinguish well-differentiated carcinoma from benign tumors (Fig. 3). However, another problem that must be resolved is how to distinguish active granulomatous diseases, such as tuberculosis, from malignancy (*8*) because they had SUV levels from 3 to 5 (4.97 ± 2.3) and an RI-SUV of 41.2%. These levels were higher than those of well-differentiated carcinoma and lower than those of poorly differentiated carcinoma. We believe that an understanding of these data as well as the results of thoracic CT scans will improve the potential accuracy for diagnosis of tuberculosis.

CONCLUSION

Our results provide further evidence that ^{18}F-FDG PET is an important noninvasive method for the differentiation of malignant and nonmalignant lesions. This imaging technique, dual-time-point ^{18}F-FDG PET imaging, has been found to be extremely helpful before surgery in patients with otherwise unclear thoracic nodules and nodal involvement.

ACKNOWLEDGMENTS

We gratefully acknowledge the support by Prof. Yasuhisa Fujibayashi and the radiopharmaceutical chemistry group at Biomedical Imaging Research Center for their valuable assistance in preparing ^{18}F-FDG.

REFERENCES

1. Coleman RE. PET in lung cancer. *J Nucl Med.* 1999;40:814–820.
2. Prauer HW, Weber WA, Romer W, et al. Controlled prospective study of positron emission tomography using the glucose analogue [^{18}F]fluorodeoxyglucose in the evaluation of pulmonary nodules. *Br J Surg.* 1998;85:1506–1511.
3. Bar-Shalom R, Valdivia AY, Blaufox MD. PET imaging in oncology. *Semin Nucl Med.* 2000;30:150–185.
4. Nunan TO, Hain SF. PET in oncology. 2. Other tumors. *Nucl Med Commun.* 2000;21:229–223.

5. Conti PS, Lilien DL, Hawley K, et al. PET and [18F]-FDG in oncology: a clinical update. *Nucl Med Biol.* 1996;23:717–735.
6. Kapucu LO, Meltzer CC, Townsend DW, et al. Fluorine-18-fluorodeoxyglucose uptake in pneumonia. *J Nucl Med.* 1998;39:1267–1269.
7. Lewis PJ, Salama A. Uptake of fluorine-18-fluorodeoxyglucose in sarcoidosis. *J Nucl Med.* 1994;35:1653–1655.
8. Jin MC, Jung-Gi I, Kyung-Hyun D, et al. Pulmonary tuberculoma evaluated by means of FDG-PET: findings in 10 cases. *Radiology.* 2000;216:117–121.
9. Pitman AG, Hicks RJ, Kalff V, et al. Positron emission tomography in pulmonary masses where tissue diagnosis is unhelpful or not possible. *Med J Aust.* 2001; 175:303–307.
10. Sazon DA, Santiago SM, Soo Hoo GW, et al. Fluorodeoxyglucose-positron emission tomography in the detection and staging of lung cancer. *Am J Respir Crit Care Med.* 1996;153:417–421.
11. Chin BB, Zukerberg W, Buchpiguel C, et al. Thallium-201 uptake in lung cancer. *J Nucl Med.* 1995;36:1514–1519.
12. Kohei Y, Okuyama A, Mori K, et al. Mediastinal lymph node metastasis from lung cancer: evaluation with T-201 SPECT—comparison with CT. *Radiology.* 1994;192:813–817.
13. Takekawa H, Itoh K, Abe S, et al. Thallium-201 uptake, histopathological differentiation and Na-K ATPase in lung adenocarcinoma. *J Nucl Med.* 1996;37: 955–958.
14. Imadahl A, Nitzsche E, Krautmann F, et al. Evaluation of positron emission tomography with 2-[18F]fluoro-2-deoxy-D-glucose for the differentiation of chronic pancreatitis and pancreatic cancer. *Br J Surg.* 1999;86:194–199.
15. Boemer AR, Weckesser M, Herzog H. Optimal scan time for fluorine-18 fluorodeoxyglucose positron emission tomography in breast cancer. *Eur J Nucl Med.* 1999;26:226–230.
16. Kubota K, Itoh M, Ozaki K, et al. Advantage of delayed whole-body FDG-PET imaging for tumor detection. *Eur J Nucl Med.* 2001;28:696–703.
17. Zhuang H, Pourdehnad M, Lambright ES, et al. Dual time point 18F-FDG PET imaging for differentiating malignant from inflammatory processes. *J Nucl Med.* 2001;42:1412–1417.
18. Matthies A, Hickeson M, Cuchiara A, et al. Dual time point 18F-FDG PET for the evaluation of pulmonary nodules. *J Nucl Med.* 2002;43:871–875.
19. Hamberg LM, Hunter GJ, Alpert NM, et al. The dose uptake ratio as an index of glucose metabolism: useful parameter or oversimplification? *J Nucl Med.* 1994; 35:1308–1312.
20. Liewarld F, Grosse S, Storck M, et al. How useful is positron emission tomography for lymph node staging in non-small-cell lung cancer? *Thorac Cardiovasc Surg.* 2000;48:93–96.
21. Younes M, Lechgo L, Somoano JR, et al. Wide expression of the human erythrocyte glucose transporter Glut 1 in human cancers. *Cancer Res.* 1996;56: 1164–1167.
22. Gallagher BM, Fowler JS, Gutterson NI, et al. Metabolic trapping as a principle of radiopharmaceutical design: some factors responsible for the biodistribution of [18F] 2-deoxy-2-fluoro-D-glucose. *J Nucl Med.* 1978;19:1154–1161.
23. Nelson CA, Wang JQ, Leav I, et al. The interaction among glucose transport, hexokinase, and glucose-6-phosphatase with respect to 3H-2-deoxyglucose retention in murine tumor models. *Nucl Med Biol.* 1996;23:533–541.
24. Suzuki S, Toyota T, Suzuki H, et al. Partial purification from human mononuclear cells and placental plasma membranes of an insulin mediator which stimulates pyruvate dehydrogenase and suppresses glucose-6-phosphatase. *Arch Biochem Biophys.* 1984;235:418–426.
25. Gupta N, Gill H, Graeber G, et al. Dynamic positron emission tomography with F-18 fluorodeoxyglucose imaging in differentiation of benign from malignant lung/mediastinal lesions. *Chest.* 1998;114:1105–1111.
26. Higashi K, Clavo AC, Wahl RL. Does FDG uptake measure proliferative activity of human canser cells? in vitro comparison with DNA flow cytometry and tritiated thymidine uptake. *J Nucl Med.* 1993;34:414–419.
27. Duhaylongsod FG, Lowe VJ, Patz EF, et al. Lung tumor growth correlates with glucose metabolism measured by fluoride-18 fluorodeoxyglucose positron emission tomography. *Ann Thorac Surg.* 1995;60:1348–1352.
28. Lowe VJ, Fletcher JW, Gobar L, et al. Prospective investigation of positron emission tomography in lung nodules. *J Clin Oncol.* 1998;16:1075–1084.
29. Lowe VJ, Hoffman JM, Delong DM, et al. Semiquantitative and visual analysis of FDG-PET images in pulmonary abnormalities. *J Nucl Med.* 1994;35:1771–1776.
30. Larson SM. Cancer or inflammation? a holy grail for nuclear medicine. *J Nucl Med.* 1994;35:1647–1649.
31. Kubota K, Matsuzawa T, Fujiwara T, et al. Differential diagnosis of lung tumor with positron emission tomography: a prospective study. *J Nucl Med.* 1990;31: 1927–1933.
32. Higashi K, Ueda Y, Sakuma T, et al. Comparison of [18F]FDG PET and 201Tl-SPECT in evaluation of pulmonary nodules. *J Nucl Med.* 2001;42:1489–1496.

JNM The Journal of NUCLEAR MEDICINE

^{18}F-FDG Accumulation with PET for Differentiation Between Benign and Malignant Lesions in the Thorax

Yoshiki Demura, Tatsuro Tsuchida, Takeshi Ishizaki, Shiro Mizuno, Yoshitaka Totani, Shingo Ameshima, Isamu Miyamori, Masato Sasaki and Yoshiharu Yonekura

J Nucl Med. 2003;44:540-548.

The Journal of Nuclear Medicine is published monthly.
SNMMI | Society of Nuclear Medicine and Molecular Imaging
1850 Samuel Morse Drive, Reston, VA 20190.
(Print ISSN: 0161-5505, Online ISSN: 2159-662X)

SNMMI SOCIETY OF NUCLEAR MEDICINE AND MOLECULAR IMAGING